journal

J. Am. Ceram. Soc., **89** [1] 230–235 (2006)
DOI: 10.1111/j.1551-2916.2005.00666.x

Preparation of Ultra-Fine Nickel Manganite Powders and Ceramics by a Solid-State Coordination Reaction

Dao-lai Fang, Zhong-bing Wang, Ping-hua Yang, Wei Liu, and Chu-sheng Chen[†]

Laboratory of Advanced Functional Materials and Devices, Department of Materials Science and Engineering, University of Science and Technology of China, Hefei, Anhui 230026, China

A. J. A. Winnubst

Laboratory for Inorganic Materials Science, University of Twente, MESA$^+$ Institute of Nanotechnology, P.O. Box 217, 7500 AE Enschede, The Netherlands

A solid-state coordination reaction was adopted to prepare negative temperature coefficient ceramics. A mixed oxalate $NiMn_2(C_2O_4)_3 \cdot 6H_2O$, a coordination compound, was synthesized by milling a mixture of nickel acetate, manganese acetate, and oxalic acid for 5 h at room temperature. An ultrafine $NiMn_2O_4$ powder was obtained by calcining the mixed oxalate in air at 850°C for 2 h. Ceramics with a relative density of more than 97% were achieved by sintering powder compacts at a temperature as low as 1050°C for 5 h. The specific electrical resistivity $\rho_{25°C}$ and the thermal constant $B_{25°/85°C}$ were 2174 Ω · cm and 3884 K, respectively. The drift of the resistivity after aging at 150°C for 1000 h was 3.0%.

I. Introduction

THE Mn-based transition-metal spinel oxide ceramics are widely used as negative temperature coefficient (NTC) thermistors for temperature measurement and compensation due to their high sensitivity to temperature change and low price.[1–3] The specific resistivity of these ceramics follows the well-known Arrhenius relation: $\rho = \rho_0 \exp(E_a/kT)$, in which ρ is the specific resistivity, E_a is the activation energy for conduction, k is Boltzmann's constant, and T is the absolute temperature. In practice, the NTC thermistors are characterized by two parameters: B, the thermal constant (with units in Kelvin), which is related to $B = E_a/k$, and $\rho_{25°C}$, the specific resistivity at 25°C. The main problem for the ceramic NTC thermistor lies in the drift of the resistivity with time, usually called aging. It has been shown that the aging of the NTC thermistor is largely affected by the density and homogeneity of the ceramics. Therefore, synthesis of oxide powders with improved sintering activity and homogeneity is crucial for improvement of NTC thermistors.[4]

There are two main methods used for preparation of powders for NTC ceramic thermistors,[5–8] namely, solid-state processes and wet-chemical processes. The solid-state method involves mixing and milling of precursors, usually oxides or salts, at room temperatures and calcination at elevated temperatures during which the spinel structure is formed. This method has the advantages of a relatively low number of processing steps and low process costs, but the powder prepared is less active in sintering due to the high calcination temperatures used, and the homogeneity of the powder is often insufficient due to the degree of mixing. The wet-chemical method usually involves the preparation of an intermediate from a precursor solution at room temperature and calcination of the intermediate at elevated temperatures. The powder prepared by the wet-chemical process has better sintering activity and chemical homogeneity, but the method has a number of disadvantages including more and complicated processing steps and difficulty in achieving the desired stoichiometry of the powder due to the difference in solubility between various ions.

The solid-state coordination reaction method, in a certain sense, lies in between the solid-state and the wet-chemical method. In this method, a solid-state coordination compound is formed by dry milling of starting precursor powders at room temperatures,[9–11] which is then subjected to calcination at elevated temperatures to yield powders with high sintering activity and the desired stoichiometry. In this work, this method is adopted for the preparation of $NiMn_2O_4$ NTC ceramics. Furthermore, this paper describes the calcination and the sintering behavior of the prepared oxide powders. The electrical properties of the obtained NTC ceramics are also given.

II. Experimental Procedure

Analytical-grade nickel acetate $Ni(CH_3COO)_2 \cdot 4H_2O$, manganese acetate $Mn(CH_3COO)_2 \cdot 4H_2O$, and oxalic acid $H_2C_2O_4 \cdot 2H_2O$ were used as starting materials. A powder mixture with a molar ratio of Ni^{2+}:Mn^{2+}:oxalic acid of 1:2:3.3 was ball milled at room temperature for 5 h in a polyethylene container using zirconia balls as the milling medium. Zirconia balls of 15 mm and 10 mm in diameter were used with a number ratio of 1:1, and the weight ratio of the powder mixture and milling balls was 1:4. The milled mixture was then dried at 70°C and calcined for 2 h at temperatures of 400°, 550°, and 850°C. For preparation of thermistor components, powders calcined at 850°C were uniaxially pressed at 60 MPa to form disk-shaped samples with a diameter of 6 mm and a thickness of 3 mm, and then isostatically pressed at 300 MPa. These powder compacts were sintered at 1050°C for 5 h in air.

The contents of Ni and Mn ions in nickel acetate and manganese acetate, the 850°C-calcined oxide powders, and 1050°C-sintered ceramics were determined by chemical analysis, using disodium ethylene diamine tetra acetate (EDTA) as a chelator, and eriochrome Black T as an indicator. For determination of the total amount of nickel and manganese in the 850°C-calcined oxide powder or the sintered ceramics, they were dissolved in a solution of hydrochloric acid, and excess EDTA was used to chelate nickel and manganese ions at pH = 10. The superfluous EDTA was titrated using a $MnSO_4$ solution of known manganese content. For determination of individual manganese and nickel content in oxide powder or the sintered ceramics, H_2O_2 was used to oxidize manganese ions, converting manganese ions into precipitates of hydrated manganese oxides. The precipitates were filtered and washed thoroughly. The amount of nickel ions was determined by titrating the obtained filtrate. Thus, the amount of manganese ions was calculated by subtracting the

B. Ghate—contributing editor

Manuscript No. 20103. Received February 2, 2005; approved June 26, 2005.
[†]Author to whom correspondence should be addressed. e-mail: ccsm@ustc.edu.cn

amount of nickel ions from the determined total amount of nickel and manganese ions.

A Philips X'pert Pro X-ray diffractometer (Philips, the Netherlands) with Cu$K\alpha$ radiation ($\lambda = 1.5418$ Å) was used to analyze the phase compositions of the oxalate precursors, the oxide powders and the sintered ceramics. The powdered sample of the sintered ceramics was used for phase analysis of the inner part of the sintered ceramics. An as-sintered ceramic was used for phase analysis of the surface of the sintered ceramics.

Thermogravimetric analyses (TGA) of 10.740 mg of the oxalate precursors and 11.758 mg of the 350°C-calcined powders from the oxalate precursors were performed on a Shimadzu TGA-50H thermal analyzer (Shimadzu Corp., Kyoto, Japan). Prior to the experiment of TGA, the oxide powders were degassed for 3 h under vacuum ($\sim$1 Pa). The experiments were performed in an air flow at a heating rate of 10°C/min from room temperature to $\sim$900°C.

The primary particle size of the 850°C-obtained oxide powder was analyzed by using a Hitachi-800 transmission electron microscope (TEM) (Hitachi Ltd., Tokyo, Japan). The particle size distribution of the oxide powder was determined by the centrifugal sedimentation method on an NSKC-1A Particle Size Analyzer (made in Nanjing University of Technology, Nanjing, China). Prior to these measurements, a suspension of the oxide powder was prepared by ultrasonically (5 min) dispersing the powder in distilled water, using sodium hexametaphosphate as a deflocculant. For calculating the particle size, it was assumed that the particles had a spherical shape. The microstructure of the ceramic samples was analyzed by using a Hitachi X-600 scanning electron microscope (SEM).

For sintering studies, cylindrical compacts of the 850°C-calcined powder were made by isostatic pressing at 300 MPa. The length and diameter of the compacts were 8–10 and 5–6 mm, respectively. Densification of the compacts was studied using a Netzsch DIL 402C dilatometer (Netzsch, Selb, Germany) in an air flow. Linear shrinkage was recorded as a function of time while the compact was heated at a rate of 5°C/min, held for 1 h at 1050°C, and cooled at 5°C/min. The bulk densities ρ_{bulk} of the powder compacts and ceramic samples were determined by the Archimedes method in mercury, and their relative density ρ_{rel} was calculated from the formula $\rho_{rel} = \rho_{bulk}/\rho_{th}$, where ρ_{th} is the theoretical density as obtained from X-ray diffraction (XRD) data of oxide powders and ceramics.

To measure the electrical resistivity, the electrodes were mounted on the two opposite surfaces of the ceramic disks, using two different methods of metallization. The classic method usually used in industry, called "serigraphy", includes brushing silver paste (which consists of Ag powder and organic binder) on the two surfaces of the disks, annealing at 850°C for 20 min, followed by rapid cooling to room temperature. The second method implied the deposition of a thin film of silver by evaporation under vacuum ($\sim 10^{-3}$ Pa). Ag wires were attached to these disk-shaped samples for electrical measurement. The thermistor samples' resistivity at 25° and 85°C was measured with an Agilent 34401A digital multimeter (Palo Alto, CA), during which the thermistor samples were immersed in silicon oil, whose temperature fluctuation around the designated value was less than $\pm$0.05°C. The $B_{25°/85°C}$ value was calculated according to the formula $B_{25°/85°C} = 1778 \ln(R_{25}/R_{85})$, where R_{25} and R_{85} were the resistances at 25° and 85°C, respectively. The values of $B_{25°/85°C}$ and specific resistivity $\rho_{25°C}$ were the average of 10 thermistor samples, and the standard deviation was less than 1%. The aging coefficient is characterized by the relative variation $100\% \times (R - R_0)/R_0$, in which R_0 is the resistance value measured at 25°C before annealing; R is the resistance value measured at 25°C after annealing at 150°C for 1000 h.

III. Results and Discussion

(1) Formation and Thermal Decomposition of Mixed Nickel–Manganese Oxalate

Water and acetic acid appeared soon after the starting materials had been milled, indicating the occurrence of reactions. After ball milling for 5 h, a cream-like, viscous substance was formed, which was then dried at 70°C, yielding a fine powder of light green color.

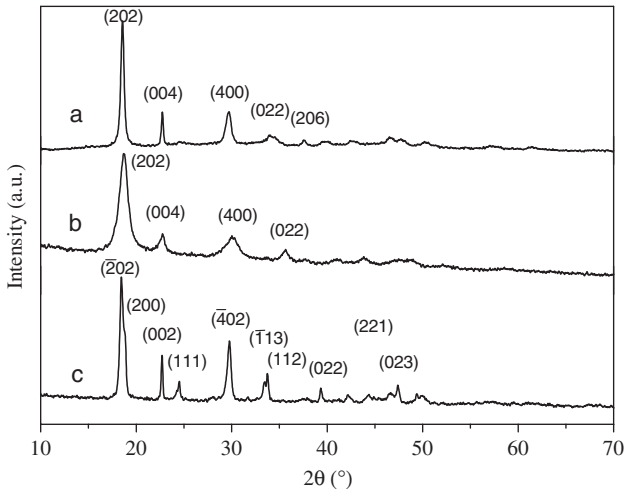

Fig. 1. X-ray diffraction patterns of the three different oxalates (a) $NiMn_2(C_2O_4)_3 \cdot nH_2O$; (b) $NiC_2O_4 \cdot nH_2O$; and (c) $MnC_2O_4 \cdot nH_2O$.

Figure 1(a) gives the XRD pattern of the dried nickel and manganese oxalate powders. For comparison, the XRD results of single nickel oxalate and manganese oxalate prepared in the same way are also given in Figs. 1(b) and (c), respectively. The XRD results show that the nickel and manganese oxalate prepared by a solid-state coordination reaction is a single-phase mixed oxalate, apparently the same as the β form nickel oxalate (JCPDS: 25-0582), distinctly different from α form manganese oxalate (JCPDS: 25-0544). The characteristic peaks of the starting acetates are not observed in the dried powder, which is an indication of the completion of the reaction.

Figure 2 shows the TGA traces of the oxalate powders. For the mixed nickel–manganese oxalate (Fig. 2(a)), two intense and sharp peaks of mass loss occur at 193.5° and 292.8°C, respectively. As to the mechanical mixture of 33% nickel oxalate and 67% manganese oxalate, four distinct mass loss peaks appear (Fig. 2(b)). The difference in the thermal decomposition behavior between a mixed nickel–manganese oxalate and a mixture of nickel and manganese oxalate has been reported in earlier works.[12,13] The results of TGA analysis clearly show that the nickel–manganese oxalate that we prepared is a single-phase mixed oxalate, rather than a mechanical mixture of nickel oxalate and manganese oxalate, consistent with the results of the XRD analysis.

Detailed examination of the TGA traces of the mixed oxalate shows that the 19.8% mass loss at 193.5°C corresponds to the dehydration of the mixed nickel–manganese oxalate $NiMn_2(C_2O_4)_3 \cdot nH_2O$, which is highly consistent with 20.0% mass loss calculated by the reaction:

$$NiMn_2(C_2O_4)_3 \cdot 6H_2O = NiMn_2(C_2O_4)_3 + 6H_2O$$

The 35.7% mass loss at 292.8°C is due to the decomposition of anhydrous oxalate; the theoretical mass loss is 37.0%, as calculated from the reaction:

$$NiMn_2(C_2O_4)_3 + 2O_2 = NiMn_2O_4 + 6CO_2$$

The deviation of experimentally found mass loss from the theoretical one is attributed to the formation of a nonstoichiometric oxide $NiMn_2O_{4+\delta}$ during decomposition of the oxalate precursors at a lower temperature ($\sim$350°C).[13,14]

For further investigation on the variation of mass and thermal stability of oxides, TGA of the oxide powders obtained by calcining the oxalate precursors for 2 h at 350°C was carried out. The TGA traces (Fig. 3) present the following three stages:

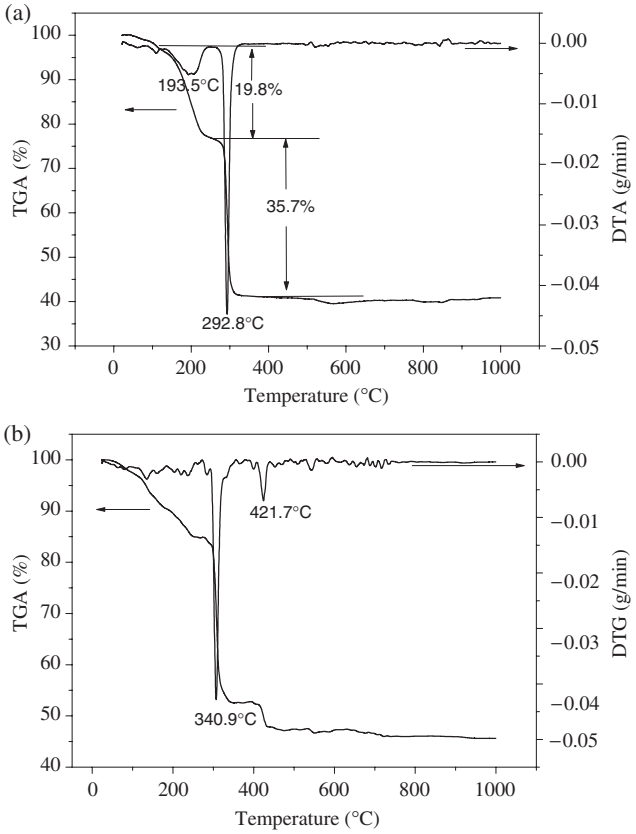

Fig. 2. Thermogravimetric analysis (TGA) and its first derivative of (a) as-prepared $NiMn_2(C_2O_4)_3 \cdot nH_2O$ and (b) a mechanical mixture of 33% nickel oxalate and 67% manganese oxalate in air flow at a heating rate of 10°C/min.

In the temperature range of 200°–506°C, successive mass loss occurs, corresponding to the loss of oxygen excess δ according to:[15]

$$NiMn_2O_{4+\delta} = NiMn_2O_4 + \delta/2O_2$$

In the temperature range of 506°–784°C, mass increases up to a temperature of about 650°C, which is related to the oxidation of Mn^{2+} into Mn^{3+} in tetragonal sites, and the decomposition of spinel phase occurs by the formation of α-Mn_2O_3 and the ilmenite $NiMnO_3$ according to the reaction:

$$2NiMn_2O_4 + 1/2O_2 = Mn_2O_3 + 2NiMnO_3$$

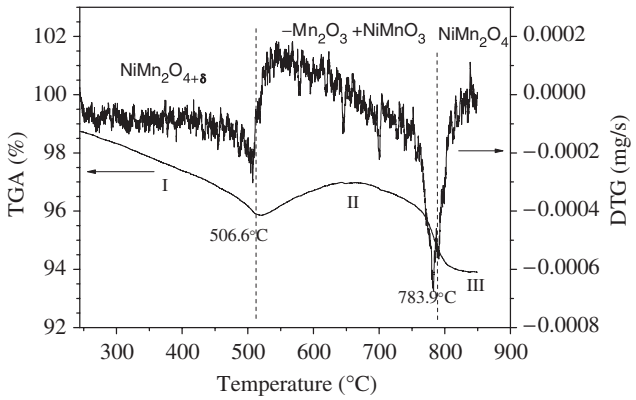

Fig. 3. Thermogravimetric analysis and its first derivative of oxide powders obtained by calcining the oxalate precursors at 350°C for 2 h in air flow at a heating rate of 10°C/min.

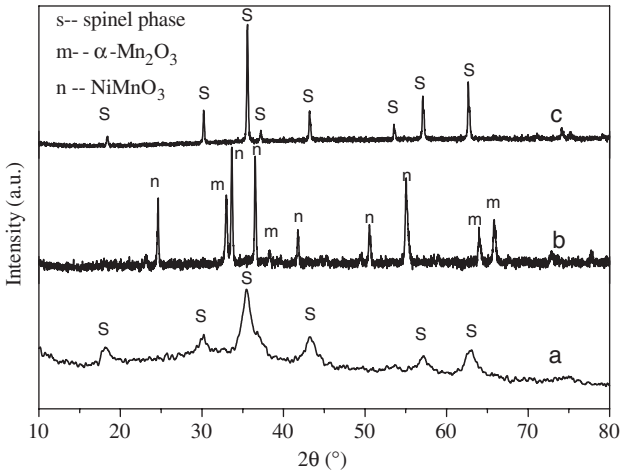

Fig. 4. X-ray diffraction patterns of oxide powders obtained by calcining oxalate precursors for 2 h at different temperatures (a) 400°C, (b) 550°C, and (c) 850°C.

However, the reverse reaction occurs at a temperature higher than 650°C, and Mn^{3+} is reduced to Mn^{2+}. Therefore, a spinel phase is formed with a remarkable mass loss.

At temperatures above 800°C, a stoichiometric spinel phase, $NiMn_2O_4$, is formed and preserved.

Figure 4 shows the XRD patterns of the powders calcined at various temperatures. Figure 4(a) shows that a mixed oxide of spinel structure is formed at a temperature of 400°C. The peak broadening indicates that the crystallites in the powders are very fine and/or that the powder is not well crystallized. The reason why the spinel can be formed at such a low temperature of 400°C is that in the mixed nickel–manganese oxalate, both nickel and manganese ions are homogeneously dispersed. It is necessary to note that when the calcination temperature is raised to 550°C, part of the spinel decomposes to α-Mn_2O_3 and the ilmenite $NiMnO_3$.[12,13] With further increase of the calcination temperature to 850°C, a single-phase spinel oxide powder is obtained, and the diffraction peaks also become sharp due to the growth of the crystallites. Therefore, the XRD result (Fig. 4) is well in agreement with that of TGA (Fig. 3).

(2) Characterization of the 850°C-Calcined Powder and the Sintering Behavior of the Powder Compacts

The chemical composition of the 850°C-calcined powder was determined by chemical analysis, and the results are listed in Table I. The molar ratio of nickel and manganese ions is 0.996:2.004, very close to the expected ratio of 1:2. In principle, the solid coordination route should cause no deviation in the resulting composition. In a sense, the stoichiometry of the resulting oxide is only determined by raw materials (e.g., purity). XRD analysis (Fig. 4(c)) indicates that the 850°C-calcined oxide is a pure spinel phase. Therefore, the chemical formula of the mixed oxide can be denoted as $Ni_{0.996\pm0.003}Mn_{2.004\pm0.005}O_4$.

The particle size distribution of the oxide powder is given in Fig. 5. The powder exhibits a narrow size distribution with a median particle size D_{50} of 0.42 μm and D_{90} of 2.0 μm, which

Table I. Properties of the 850°C-Calcined Powder

Chemical/phase composition	$Ni_{0.996\pm0.003}Mn_{2.004\pm0.005}O_4$/spinel
D_{50}/D_{90} (μm)	0.42/2.0
$d_{primary}$ (μm)	0.15
Relative density of the powder compact (%) (under isostatic pressure of 300 MPa)	63

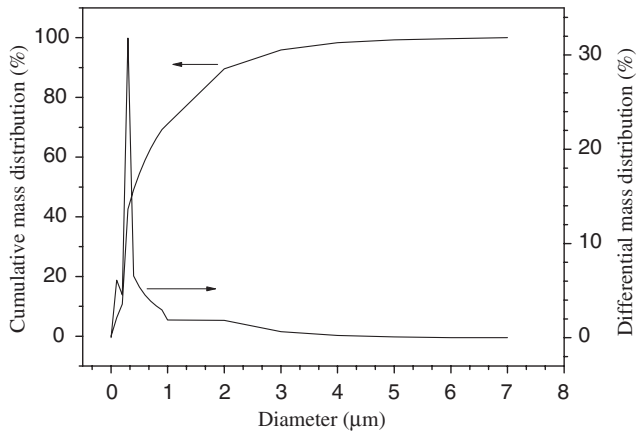

Fig. 5. Particle size distribution of the 850°C-calcined powder.

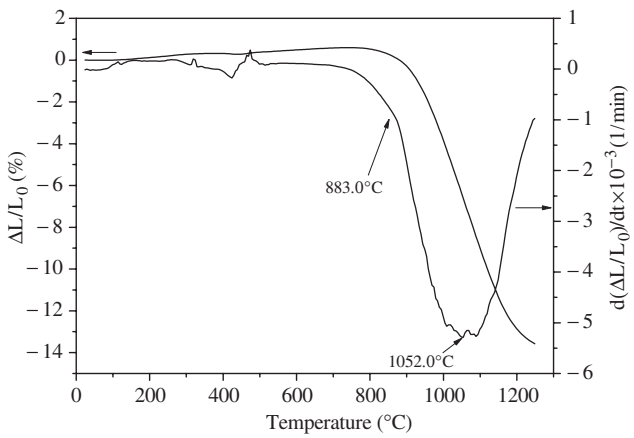

Fig. 7. Dilatometric analysis of the 850°C-calcined powders in air at a heating rate of 5°C/min.

means 50 wt% of the powder is smaller than 0.42 μm and 90 wt% of the powder is smaller than 2.0 μm in particle size. Figure 6 shows a TEM picture of the calcined powder. It can be seen that the primary particles of the powder are polygonal shaped, with a mean diameter of about 150 nm. Most of the primary particles have merged into dense aggregates with a size of about 400 nm, which is highly consistent with the results of the particle size distribution as given in Fig. 5. The narrow size distribution and the dense aggregates of small size may responsible for the high relative density (63%) of the powder compacts after isostatic pressing at 300 MPa.

Dilatometric analysis of a green compact pressed under an isostatic pressure of 300 MPa was performed in an air flow at a heating rate of 5°C/min, as shown in Fig. 7. The compact starts to shrink rapidly at about 883°C, and the shrinkage rate reaches its maximum value at about 1052°C, at which the linear shrinkage of the compact is about 8%. The shrinkage rate of the compact decreases sharply at above 1100°C, and the linear shrinkage reaches about 13.5% at a temperature of 1240°C. The presence of only one maximum in the shrinkage rate curve confirms the single mode of sintering behavior and a narrow pore size distribution in the green compact.[16]

It was observed that in the temperature range of 1000°–1100°C, the shrinkage rate maintains almost the same maximum, and the linear shrinkage increases from 3.7% to 9.1%. The results of the sintering cycle (Fig. 8) show that the isothermal sintering at 1050°C for 1h is highly effective for promoting densification of the powder compact, with the linear shrinkage increasing to 14% from 8%. After the experiment of sintering cycle, the relative density of the sintered compact was measured to be 96.5%. At the end of isothermal sintering at 1050°C for 1 h, the trend of shrinkage is retained, although the shrinkage rate decreases greatly. Therefore, one can expect that well-densified ceramics can be obtained by isothermal sintering at 1050°C for several hours. In fact, a powder compact was sintered for 5 h at 1050°C, resulting in a relative density of 97%.

Figure 9 shows an SEM picture of a fractured surface of the ceramic sintered at 1050°C for 5 h. It shows that the material is well densified and microstructurally homogeneous. In order to reach a relative density of 97%, the sintering temperature required for a powder prepared by the solid-state reaction is 200°C higher, and 110°C higher for a powder prepared by the co-precipitation method.[17,18]

A high sintering activity of mixed oxide powders is required for obtaining a well-densified single-phase ceramic, specifically for oxides like $NiMn_2O_4$, whose decomposition temperature is relatively low (950°C).[19] The XRD patterns (Figs. 10(a) and (b)) of the as-obtained ceramic surface and the powdered ceramics show no obvious difference in their phase compositions, indicating that the ceramic sintered at 1050°C for 5 h almost retains the single-phase spinel without the rocksalt phase NiO being detected, which would be present at higher sintering temperatures. The other advantage of the coordination compound route is its convenience in controlling the stoichiometry. The chemical analysis of the sintered ceramic (Table II) indicates that its

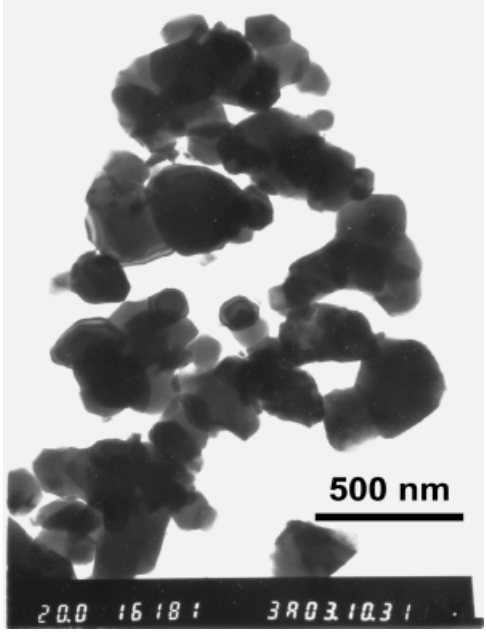

Fig. 6. Transmission electron microscope picture of the $NiMn_2O_4$ powders obtained by calcining the mixed oxalate precursors for 2 h at 850°C.

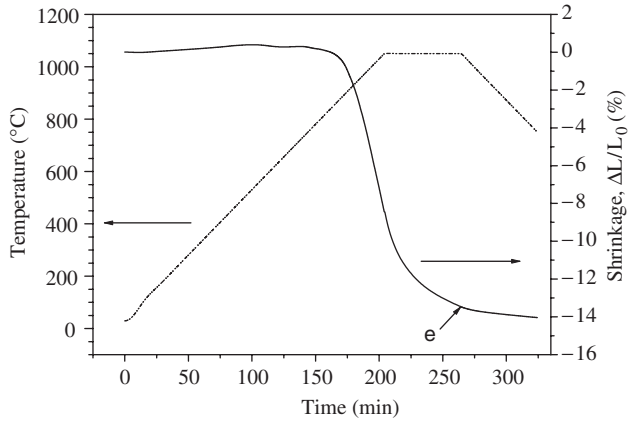

Fig. 8. Sintering cycle of the 850°C-calcined powder in air at a heating or cooling rate of 5°C/min.

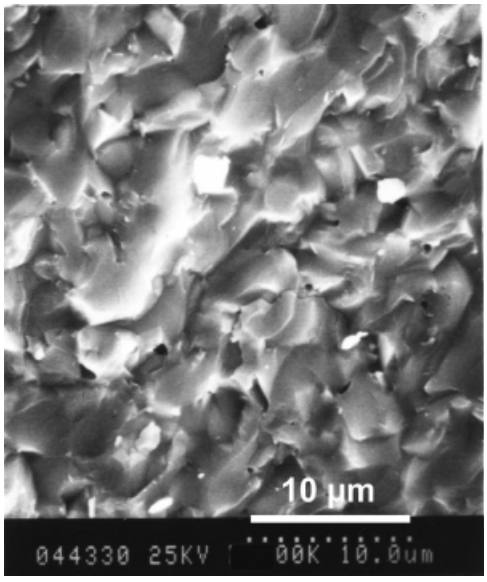

Fig. 9. Scanning electron microscope picture of a fractured surface of the ceramics sintered for 5 h at 1050°C.

chemical composition is almost similar to the one we prepared at the beginning.

(3) NTC Properties of the Resulting Ceramics

The NTC properties of the thermistor samples are listed in Table II, which are in accordance with those reported by Feltz *et al.*[20] It was observed that the metallization process remarkably influences the electrical properties. Compared with the electrical properties of the samples metallized by evaporation, the resistivity of the samples by "serigraphy" decreases by 13.5%, and the aging coefficient rises to 3.0%. The change in the electrical properties is attributed to the microstructural modification of thermistor samples caused by the metallization process of "serigraphy". The microstructural modification involves the migration of some of the Ni cations from the octahedral to the tetrahedral sites in spinel, and the oxidation and the formation of cationic defect spinel phase in the ceramic samples.[18] However, because of its convenience of forming strong adherence of electrodes to ceramics, "serigraphy" is preferable in industrial production. The instability of thermistors induced by "serigraphy" can be alleviated by subsequent annealing at 200°–600°C for several days.

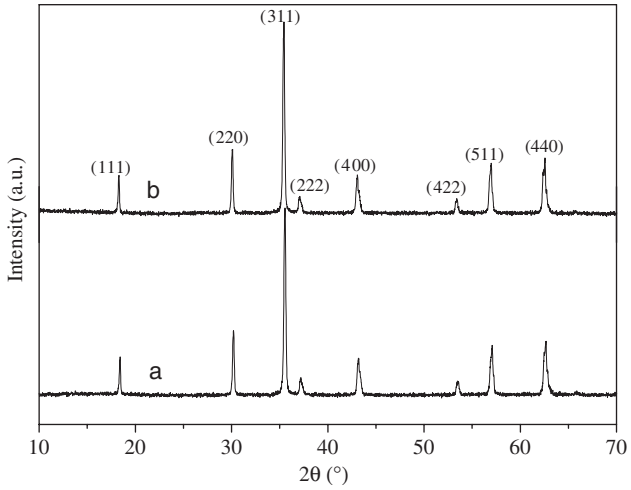

Fig. 10. X-ray diffraction patterns of $NiMn_2O_4$ ceramics sintered for 5 h at 1050°C.

Table II. Electrical Properties of $NiMn_2O_4$ Thermistor Samples

Method of metallization	Resistivity, $\rho_{25°C}$ ($\Omega \cdot$ cm)	*B* value (K)	Aging coefficient (%)
Serigraphy	2174	3884	3.0
Evaporation	2512	3912	0.5
Bulk density (g/cm^3)/ relative density (%)		5.03/97	
Chemical/phase composition		$Ni_{0.995\pm0.003}Mn_{2.005\pm0.005}O_4$/ spinel	

It should be noted that the aging coefficient of the samples metallized by "serigraphy" in our work (3.0%) is remarkably less than the result, ~10%, as reported by R. Metz.[21] This may be related to the oxide powder processing and sintering conditions. The well-densified ceramic samples that we prepared prevent the adsorption and release of oxygen; thus, the oxidization of the samples at a higher temperature (~150°C) is alleviated. As a result, the ceramic thermistor obtained shows higher stability.

IV. Conclusions

A mixed nickel and manganese oxalate can be synthesized through a solid-state coordination reaction using nickel acetate, manganese acetate, and oxalic acid as starting materials, and $NiMn_2O_4$ powders can be derived by calcination of the mixed oxalate. Dense NTC ceramics can be obtained by sintering the powder compact at a relatively low temperature of 1050°C. This work shows that the solid-state coordination reaction is a promising route to prepare mixed transition-metal oxide powders with high sintering activity and NTC ceramics with desired stoichiometry. The dense ceramic thermistor obtained shows higher stability.

References

[1]H. Okuda, "NTC Thermistors Offer Accuracy, Reliability, and Satisfy Tougher Requirements," *J. Electron. Eng.*, **32** [344] 23–6 (1995).
[2]G. Lavenuta, "Negative Temperature Coefficient Thermistors," *Sensors*, **14** [5] 46–55 (1997).
[3]R. K. Kamat and G. M. Naik, "Thermistors—in Search of New Applications, Manufacturers Cultivate Advanced NTC Techniques," *Sensor Rev.*, **22** [4] 334–40 (2002).
[4]J. G. Fagan and V. R. W. Amarkoon, "Reliability and Reproducibility of Ceramic Sensors: Part I, NTC Thermistors," *Am. Ceram. Soc. Bull.*, **72** [1] 70 (1993).
[5]C. Chanel, S Fritsch, C. Drouet, and A. Rousset, "Synthesis, Thermogravimetric and Hightemperature X-Ray Diffraction Analyses of Zinc-Substituted Nickel Manganites," *Mater. Res. Bull.*, **35** [3] 431–9 (2000).
[6]W. A. Groen, C. Metzmacher, P. Huppertz, and S. Schuurman, "Aging of NTC Ceramics in the System Mn–Ni–Fe–O," *J. Electrocream.*, **7** [2] 77–87 (2001).
[7]Z. X. Yue, J. H. Shan, X. W. Qi, X. H. Wang, J. Zhou, Z. L. Gui, and L. T. Li, "Synthesis of Nanocrystalline Manganite Powders Via a Gel Auto-Combustion Process for NTC Thermistor Applications," *Mater. Sci. Eng. B*, **99** [1–3] 217–20 (2002).
[8]D. Houivet, J. Bernard, and J. M. Haussonne, "High Temperature NTC Ceramic Resistors (Ambient–1000°C)," *J. Eur. Ceram. Soc.*, **24** [6] 1237–41 (2004).
[9]X. R. Ye, D. J. Jia, J. Q. Yu, X. Q. Xin, and Z. Xue, "One Step Solid-State Reactions at Ambient Temperatures—A Novel Approach to Nanocrystal Synthesis," *Adv. Mater.*, **11** [11] 941–3 (1999).
[10]J. F. Xu, W. Ji, Z. X. Shen, and S. H. Tang, "Preparation and Characterization of CuO Nanocrystals," *J. Solid State Chem.*, **147** [2] 516–9 (1999).
[11]F. Li, J. Q. Xu, X. H. Yu, L. Y. Chen, and X. Q. Xin, "One-Step Solid State Reaction Synthesis and Gas Sensing Property of Tin Oxide Nanoparticles," *Sensors Actuators B*, **81** [2–3] 65–9 (2002).
[12]C. Drouet, P. Alphonse, and A. Rousset, "Synthesis and Characterization of Nonstoichiometric Nickel–Copper Manganites," *Solid State Ions*, **123** [1–4] 25–37 (1999).
[13]C. Laberty, P. Alphonse, J. J. Demai, C. Sarda, and A. Rousset, "Synthesis and Characterization of Nonstoichiometric Nickel Manganite $Ni_xMn_{3-x}O_{4+\delta}$," *Mater. Res. Bull.*, **32** [2] 249–61 (1997).
[14]C. Laberty, J. Pielaszek, P. Alphonse, and A. Rousset, "Characterization of Nonstoichoimetric Nickel Manganite Spinels $Ni_xMn_{3-x\ 3\delta/4}\ O_{4+\delta}$ by Temperature Programmed Reduction," *Solid State Ionics*, **110** [3–4] 293–302 (1998).

[15]C. Chanel, S. Fritsch, C. Drouet, and A. Rousset, "Synthesis, Thermogravimetric and High Temperature X-Ray Diffraction Analyses of Zinc-Substituted Nickel Manganites," *Mater. Res. Bull.*, **35** [3] 431–9 (2000).

[16]P. Duran, M. Villegas, F. Capel, P. Recio, and C. Moure, "Low-Temperature Sintering and Microstructural Development of Nanocrystalline Y-TZP Powders," *J. Eur. Ceram. Soc.*, **16** [9] 945–52 (1996).

[17]G. D. C. Csete de GyoÈ rgyfalva, A. N. Nolte, and I. M. Reaney, "Correlation Between Microstructure and Conductance in NTC Thermistors Produced from Oxide Powders," *J. Eur. Ceram. Soc.*, **19** [6–7] 857–60 (1999).

[18]S. Fritsch, J. Sarrias, M. Brieu, J. J. Couderc, J. L. Baudour, E. Snoeck, and A. Rousset, "Correlation Between the Structure the Microstructure and the Electrical Properties of Nickel Manganite Negative Temperature Coefficient (NTC) Thermistors," *Solid State Ionics*, **109** [3–4] 229–37 (1998).

[19]D. G. Wickham, "Solid Phase Equilibria in the System NiO–Mn_2O_3–O_2," *J. Inorg. Chem.*, **26**, 1369–77 (1964).

[20]A. Feltz, J. Topfer, and F. Schirrmeister, "Conductivity Data and Preparation Routes for $NiMn_2O_4$ Thermistor Ceramics," *J. Eur. Ceram. Soc.*, **9** [3] 187–91 (1992).

[21]R. Metz, "Electrical Properties of N.T.C. Thermistors Made of Manganite Ceramics of General Spinel Structure: $Mn_{3-x-x'}M_xN_{x'}O_4$ ($0<-x+x'<-1$; M and N being Ni, Co or Cu) Aging Phenomenon Study," *J. Mater. Sci.*, **35** [18] 4705–11 (2000). □